

Photovoltaic performance of p-Si/Cd_{1-x}Zn_xO heterojunctions

Huseyn M. Mamedov,^{*1} Syed Ismat Shah,² Archil Chirakadze,³ Vusal U. Mammadov,¹
Vusala J. Mammadova¹ and Khumar M. Ahmedova¹

¹Baku State University, Az1148, Z.Khalilov str., 23, Baku, Azerbaijan

²University of Delaware, 208 DuPont Hall, Newark, DE 19716, USA

³Georgian Technical University, 77, Merab Kostava Street, 0175 Tbilisi, Georgia

Received February 20, 2018; accepted March 26, 2018; published March 31, 2018

Abstract—Heterojunctions of p-Si/Cd_{1-x}Zn_xO were synthesized by depositing Cd_{1-x}Zn_xO films on p-Si substrates electrochemically. The morphological properties of the films were studied by scanning microscopy. The electric and photoelectrical properties of heterojunctions were investigated depending on deposition potential and films composition. Heterojunctions of p-Si/Cd_{1-x}Zn_xO, which were deposited at a cathode potential of -1.2V, show good rectification ($k \approx 1640$). Under AM1.5 conditions, the maximal values of open-circuit voltage, short-circuit current, fill factor and efficiency of our best nanostructured cell, were $U_{oc}=442\text{mV}$, $J_{sc}=19.9\text{mA/cm}^2$, $FF=0.59$ and $\eta=5.1\%$, respectively.

Thin films of ZnO are one of the favourable materials for the production of opto- and photoelectronic devices [1-3]. CdO films are conductive, transparent in the visible region with a direct band gap of 2.5eV, being useful for solar cells, gas sensors, windows, and thin-film resistors [4-6], most importantly, show low resistance. Therefore, the resistivity of ZnO can be decreased by alloying it with CdO. The creation of solid solutions on the basis of various metal oxides and chalcogenides allows changing the physical properties and band gap of thin films, which is important at designing photonic devices of high performance in various spectral ranges [7-13]. A variety of methods have been reported for the preparation of CdO-ZnO alloy films such as molecular beam epitaxy [14], sol-gel process [15] and spray pyrolysis [16]. Among these methods, electrodeposition is an attractive method to obtain these kinds of films [17], which is well known due to its simplicity, reproducibility and possibility of producing cheap large-area films [9-13]. Although pure ZnO and CdO films have been studied by many research groups, a compound semiconductor of ZnO and CdO, that is to say Cd_{1-x}Zn_xO, has seldom been studied.

In this work, we present the electrical and photoelectrical properties of p-Si/Cd_{1-x}Zn_xO heterojunctions deposited by electrodeposition onto *glass/Al/p-Si* as substrates.

The electrochemical deposition of Cd_{1-x}Zn_xO films has been performed with a three electrode configuration: graphite electrode as anode, Ag/AgCl₃ electrode as

reference electrode and vacuum evaporated p-Si thin films (2.5Ω·cm resistivity and 200μm thickness) onto the *glass/Al* substrates as a cathode. For SEM, energy dispersive spectra (EDS), electrical and optical measurements, we used *glass/SnO₂* substrates. The total area of working electrodes (cathode) was 1×1cm². The *glass/Al/p-Si* substrates were cleaned with ethanol, acetone and deionized water and then dried in flowing N₂. At electrodeposition, we used aqueous solutions of Zn(NO₃)₂ and Cd(NO₃)₂ salts (99.5% purities) with a different molar fraction in the solution (Table 1). The solution was continuously stirred for 1 hour and then filtered by filter paper. The solution was homogeneous, clear, transparent and stable at room temperature. The reaction temperature was kept at 80°C. The thickness of Cd_{1-x}Zn_xO films was about 100÷500 nm, depending on deposition duration. Hall Effect measurements showed that the resistivity of films was 2×10⁻³÷170 Ω·cm and the free electron concentration was $n = 6.5 \times 10^{17} \div 8 \times 10^{14} \text{ cm}^{-3}$, depending on the Zn content. EDS data were recorded to determine the composition of Cd and Zn in deposited layers.

In order to fabricate heterojunctions, an Ohmic In (or Au) electrode, in a reticulose form was evaporated on the Cd_{1-x}Zn_xO films with an area of ~0.62cm². Aluminium (Al) was evaporated on the back side of the *p-Si* wafer as an Ohmic electrode, followed by annealing at 500°C in vacuum for 20 min.

It is established that the morphology of Cd_{1-x}Zn_xO films depends on the deposition potential. SEM images of films Cd_{0.4}Zn_{0.6}O deposited at -0.9V, -1.2V, -1.28 V and -1.35 V are shown in Fig. 1. The morphology of films deposited at -0.9 V is a homogeneous micro-texture structure (Fig. 1a). The SEM images showed that the size of the crystallites decreased with an increasing deposition potential from -0.9 V to -1.2 V and the films demonstrate a nanostructure surface (Fig. 1b). The particle size and shape distribution look more uniform compared to films deposited at other potentials. The uniformity in particles shape is due to higher nucleation rate and uniform particle growth. The concentration of surface defects increases by

* E-mail: mhhuseyng@gmail.com; mhhuseyng@bsu.az

increasing the deposition potential from -1.28 to -1.32 V (Fig. 1c). Future growth of potential ($U > -1.34$ V) leads to an increase of non-homogeneity degree at the surface, with films showing poor adhesion to the surface (Fig. 1d).

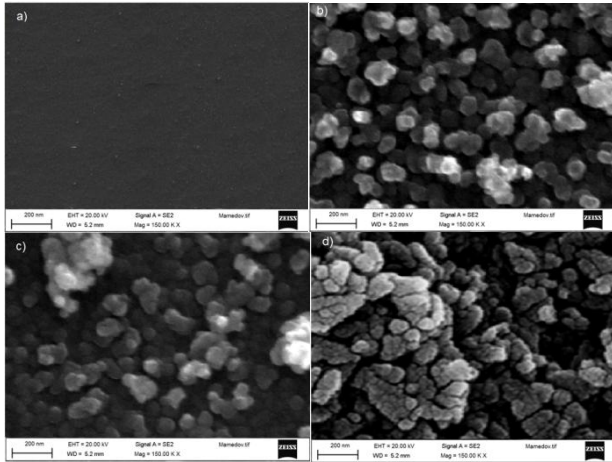


Fig. 1. SEM images of films $\text{Cd}_{0.4}\text{Zn}_{0.6}\text{O}$ deposited at -0.9 V (a), -1.2 V (b), -1.28 V (c) and -1.35 V (d).

$\text{Cd}_{1-x}\text{Zn}_x\text{O}$ thin films deposited on *glass/SnO₂* substrates show high transmission in the visible and UV range with average transmission ranging between $52 \div 93\%$ with a variation of cathode potential, showing that films can be used as transparent window materials in many opto- and photo- electronic devices. Films deposited at -0.9 V show not sharp and complicated absorption edge in the short wavelength range. It shows that the films deposited at -0.9 V contain not one, and a few crystal phases (segregation of the phases) [18]. A higher transmission value (93%) was observed for samples prepared at -1.2 V. The linear dependence of $(ah\nu)^2$ to $h\nu$ indicates that $\text{Cd}_{0.4}\text{Zn}_{0.6}\text{O}$ films are direct transition type semiconductors. The films deposited at -1.35 V show again a complicated absorption edge and little transmittance (65%) because of crystal phase segregations or high scattering in the films. The band gap (E_g) of the $\text{Cd}_{1-x}\text{Zn}_x\text{O}$ films deposited at -1.2 V was determined from extrapolation of the straight line section of the $(ah\nu)^2$ versus $h\nu$ curves (Table 1). The bandgap calculated above was found to decrease linearly from 2.95 eV ($x=0.6$) to 2.64 eV ($x=0.2$) as a function of Zn concentration. The calculated values of the band gap are found in good agreement with the values of the band gap reported in [7, 18].

The dark current-voltage (J - V) curves of the heterojunctions deposited at -1.2 V, were measured in the direct and reverse current modes. The experimental J - V curves, measured at 300 K, for a $\text{p-Si}/\text{Cd}_{1-x}\text{Zn}_x\text{O}$ heterojunction using various values of x were definitely of the diode type, with a forward direction corresponding to

the positive potential on p-Si . Built-in potential (V_{bi}), series resistance (R_s), ideality factor (n) and rectification factor (k) of heterojunctions depending on the Zn content were determined from J - V curves and summarized in Table 1.

Table 1. Electrical parameters of heterojunctions $\text{p-Si}/\text{Cd}_{1-x}\text{Zn}_x\text{O}$ deposited at -1.2 V, depending on the Zn content.

x	E_g (eV)	n	V_{bi} (V)	V_c (V)	R_s (k Ω)	k
0.2	2.64	2.4	0.44	0.48	0.01	190
0.4	2.82	2.1	0.49	0.51	0.03	246
0.5	2.91	1.79	0.56	0.52	0.05	983
0.6	2.95	1.74	0.56	0.55	0.03	1640
0.7	3.04	1.96	0.56	0.57	2	480
0.9	3.14	2.63	0.59	0.62	40	235

As seen from Table 1, the series resistance of heterojunctions increases with the Zn content, which is due to the increase of $\text{Cd}_{1-x}\text{Zn}_x\text{O}$ films resistance. However, there is non-linear dependence of rectification coefficient and ideality factor on the Zn content.

The minimum value of ideality factor is observed in heterojunctions with $x=0.6$ (Table 1), which show close lattice constants of the Si and $\text{Cd}_{0.4}\text{Zn}_{0.6}\text{O}$. Rectification in junctions with $x=0.6$ reaches the value of $k=1640$ at ± 1.5 V (Table 1). It must be noted that rectification in heterojunctions on the basis of $\text{Cd}_{1-x}\text{Zn}_x\text{O}$ for all Zn content is much higher than that reported for $\text{p-Si}/\text{ZnO}$ [19-21].

The forward current of heterojunctions with $x \neq 0.6$, is significantly dependent on the Zn content. The J - V plots of these junctions reveal two regions, having two different slopes, which sharply depend on temperature. In addition, the value of cut-off voltage (V_c) determined from C - V characteristics is less in comparison with the built-in potential (V_{bi}), determined from the linear section of J - V curves measured at room temperature (Table 1). The observed effect in heterojunctions can be explained by the dependence of relaxation times of surface states on the frequency of an alternating signal [22, 23]. However, J - V plots of junctions with $x=0.6$, reveal only one region. It is established that the linear region of the dependence $\ln I = f$ (V) does not depend on temperature, which indicates the possibility of a tunneling mechanism of current passage. However, at low applied voltages the space-charge region is not thin enough for direct tunneling. The concentration of surface states, associated with the lattice mismatch between Si and $\text{Cd}_{0.4}\text{Zn}_{0.6}\text{O}$, were calculated using the method described in [24], which is about $n \approx 6 \times 10^{15} \text{ cm}^{-3}$. Therefore, it is possible to consider a multistage tunnel-recombination mechanism of current passage, with participation of surface states at the interface.

Table 2. Photoelectrical parameters of heterojunctions p-Si/Cd_{1-x}Zn_xO deposited at -1.2 V, depending on the Zn content.

Samples <i>x</i>	U_{oc} (mV)	J_{sc} (mA/cm ²)	FF	η , %
0.2	162	14.4	0.44	1.03
0.4	263	13.8	0.51	1.85
0.5	403	13.2	0.51	2.71
0.6	442	19.9	0.59	5.1
0.7	380	8.4	0.48	1.53
0.9	320	6.8	0.45	0.98

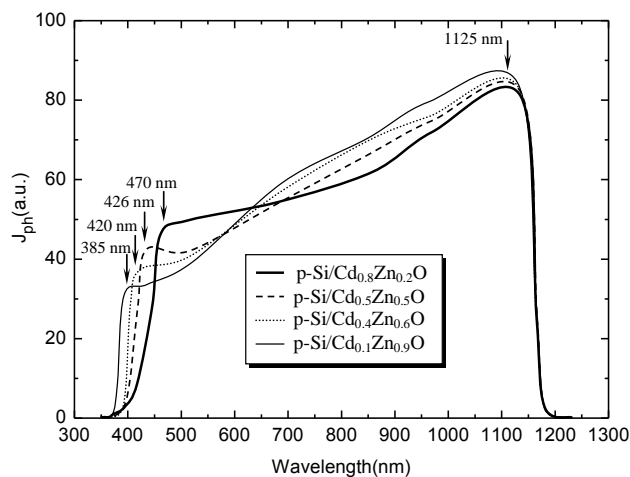


Fig. 2. Spectral distribution of photocurrent for heterojunctions p-Si/Cd_{1-x}Zn_xO with different Zn content.

Under standard test conditions, all investigated heterojunctions demonstrated photovoltaic performance, the sign of which is that open circuit photo-voltage (U_{oc}) does not change in all the region of photosensitivity. However, the maximum values of U_{oc} and J_{sc} non-monotonically depend on the Zn content. The maximum values of U_{oc} and J_{sc} were observed for heterojunctions with $x=0.6$ (Table 2). We investigated the spectral distribution of photocurrent (J_{ph}) depending on the Zn content, in a wavelength range of 200÷1300nm (Fig. 2). Near infrared photosensitivity falloff for all heterojunctions indicated Si absorber band gaps of 1125 nm. A drastically different spectral response is observed under illumination of heterojunctions from the other side, which gives rise to a short wavelength peak in the spectral dependence of photocurrent. With an increasing x , the short wavelength peak shifts to shorter wavelengths, which is attributed to the increase in the band gap of Cd_{1-x}Zn_xO and intensity of peaks decrease with x . At $x=0.6$, the peak being observed at 420nm (Fig. 2).

Thus, electrical and photoelectrical parameters of heterojunctions p-Si/Cd_{1-x}Zn_xO can be controlled by Cd_{1-x}Zn_xO films composition and deposition potential. Heterojunctions with $x=0.6$, deposited at -1.2V with a nano-structured surface show the best photoelectric

parameters: under AM1.5 conditions, maximal values of open-circuit voltage, short-circuit current, fill factor and efficiency of our best cell, which were $U_{oc}=442\text{mV}$, $J_{sc}=19.9\text{ mA/cm}^2$, $FF=0.59$ and $\eta=5.1\%$, respectively.

References

- [1] X. Li *et al.*, J. Appl. Phys. **105**, 103914 (2009).
- [2] X. Han, K. Han, M. Tao, ECS Trans. **25**, 93 (2010).
- [3] W. Liu *et al.*, J. Am. Chem. Soc. **132**, 2498 (2010).
- [4] R.A. Ismail, O.A. Abdulrazaq, Sol. Energy Mater. Sol. Cells, **91**, 903 (2007).
- [5] R.S. Mane, H.M. Pathan, C.D. Lokhande, S.H.Han, Sol. Energy **80**, 185 (2006).
- [6] E. Martin *et al.*, Thin Solid Films **461**, 309 (2004).
- [7] Y. Caglar, M. Caglar, S. Ilican, A. Ates, J. Phys. D: Appl. Phys. **42**, 065421 (2009).
- [8] F. Wang, Z. Ye, D. Ma, L. Zhu, F. Zhuge, J. Cryst. Growth, **283**, 373 (2005).
- [9] A. Abdinov, H. Mamedov, S. Amirova, Jpn. J. Appl. Phys. **46**, 7359 (2007).
- [10] A. Abdinov, H. Mamedov, H. Hasanov, S. Amirova, Thin Solid Films, **480-481**, 388 (2005).
- [11] A. Abdinov, H. Mamedov, S. Amirova, Thin Solid Films, **511-512**, 140 (2006).
- [12] H. Mamedov, V. Mamedov, V. Mamedova, Kh. Ahmadova, J. Optoelectrom. Adv. M. **17**, 67 (2015).
- [13] H. Mamedov *et al.*, J. Solar Energy Eng. **136**, 044503 (2014).
- [14] S. Sadofev, S. Blumstengel, J. Cui, J. Puls, S. Rogaschewski, P. Schafer, F. Henneberger, Appl. Phys. Lett. **89**, 201907 (2006).
- [15] G. Torres-Delgado *et al.*, Adv. Funct. Mater. **12**, 129 (2002).
- [16] H. Tabet-Derraz, N. Benramdane, D. Nacer, A. Bouzidi, M. Medles, Sol. Energy Mater. Sol. Cells **73**, 249 (2002).
- [17] M. Tortosa, M. Mollar, B. Mari, J. Cryst. Growth, **304**, 97 (2007).
- [18] A. Singh, D. Kumar, P.K. Khanna, M. Kumar, B. Prasad, ECS J. Solid State Science and Techn. **2** (9), Q136 (2013).
- [19] F.Z. Bedia, A. Bedia, B. Benyoucef, S.Hamzaoui, Phys. Procedia, **55**, 61 (2014).
- [20] M. Jing-Jing *et al.*, Chin. Phys. Lett. **27** (10), 107304 (2010).
- [21] T. Xiao-Yun, W. Yan-Hua, Y. Wei, G. Wei, F. Guang-Sheng, Chin. Phys. B **21** (9), 097105 (2012).
- [22] I. Balberg, J. Appl. Phys. **58**, 2603 (1985).
- [23] P. Chattopadhyay, D.P. Haldar, Appl. Surf. Sci. **171**, 207 (2001).
- [24] V.P. Makhniy, S.V. Khusnutdinov, V.V. Gorley, Acta Phys. Polon. A, **116**, 859 (2009).